The synthesis of heteronuclear clusters containing cyclopentadienyl- or pentamethylcyclopentadienyliridium and ruthenium or osmium

Padmamalini Srinivasan, Weng Kee Leong *

Department of Chemistry, National University of Singapore, Kent Ridge, Singapore 119260, Singapore

Abstract

The reaction of $Cp*Ir(CO)_2$ or $CpIr(CO)_2$ with $Ru_3(CO)_{12}$ under a hydrogen atmosphere afforded the heterometallic clusters $Cp*Ir-Ru_3(\mu-H)_2(CO)_{10}$ and $CpIrRu_3(\mu-H)_2(CO)_{10}$, respectively, in moderate yields. In the former reaction, the tetrahydrido cluster $Cp*Ir-Ru_3(\mu-H)_4(CO)_9$ was also formed in trace amounts, although this cluster can be obtained in high yields by the hydrogenation of $Cp*IrRu_3(\mu-H)_2(CO)_{10}$; the Cp analogue was not obtainable. The reaction of $Os_3(\mu-H)_2(CO)_{10}$ with $Cp*Ir(CO)_2$ afforded the osmium analogue $Cp*IrOs_3(\mu-H)_2(CO)_{10}$ in 70% yield, along with a trace amount of the pentanuclear cluster $Cp*IrOs_4(\mu-H)_2(CO)_{13}$. Hydrogenation of $Cp*IrOs_3(\mu-H)_2(CO)_{10}$ afforded $Cp*IrOs_3(\mu-H)_4(CO)_9$ in excellent yield. The reaction of $Cp*Ir(CO)_2$ with $Os_3(CO)_{10}(CH_3CN)_2$ afforded the known trinuclear cluster $Cp*IrOs_2(CO)_9$ and the novel cluster $Cp*IrOs_3(CO)_{11}$. Solution-state NMR studies show that the hydrides in the iridium–ruthenium clusters are highly fluxional even at low temperatures while those in the iridium–osmium clusters are less so.
© 2005 Published by Elsevier B.V.

Keywords: Iridium; Ruthenium; Osmium; Heteronuclear; Cluster; Cyclopentadienyl; Fluxional

1. Introduction

The synthesis of heteronuclear clusters continue to attract significant interest stimulated by their possible catalytic potential [1]. The combination of different metals in the same complex may also induce novel forms of substrate activation thus giving rise to interesting chemistry [2]. We have been interested in heteronuclear clusters containing metals that are diverse in chemistry, and we are also interested in those containing metals that are similar in some respects. Heteronuclear clusters containing osmium or ruthenium with iridium belong to the latter class. The use of osmium-based clusters is motivated by the stability it imparts to the cluster core and there have been a number of reports on triosmium-based mixed-metal clusters [3]. Ruthenium is well-known to be involved in a very large number of novel catalytic reactions [4], while iridium is also

important as a catalyst and in C–H activation [5]. It was therefore of interest to look at the chemistry of such heteronuclear clusters.

Although the chemistry of mixed metal platinum group metals have been extensively studied, a greater proportion of these studies have involved clusters of Ru, Pd and Pt mixed metal framework. Tetrahedral clusters containing Rh, Os, Ir or Ru mixed metal framework have been less extensively studied. Very few clusters containing a Ru_3Ir or Os_3Ir mixed metal frame work have been reported in the literature. Some of these include the very high yield synthesis of the carbonyl cluster anions $[Ru_3Ir(CO)_{13}]^-$ and $[Os_3Ir(CO)_{13}]^-$ by a redox condensation reaction [6], and via salt elimination reactions to yield several Ru–Ir mixed metal clusters [7]. There are even fewer reports on the syntheses of tetrahedral clusters with a Cp or Cp*-containing iridium–osmium or iridium–ruthenium framework [8]. On the other hand, we have found from our studies on a ruthenium–osmium system that if the two metals have great similarities then that can give rise to very complex mixtures of

* Corresponding author.
  E-mail address: chmlwk@nus.edu.sg (W.K. Leong).

isomers [9]; this was also the case in the other studies on the ruthenium–iridium clusters [7]. We have therefore endeavoured, in the osmium–iridium system, to introduce a Cp* onto the iridium as a means of differentiating it from the osmium atoms. In this paper, we report our attempts at the synthesis, and the structures, of some Cp*-containing triosmium–iridium tetrahedral clusters.

2. Results and discussion

2.1. Iridium–ruthenium clusters

The only previously known cyclopentadienyl-containing $IrRu_3$ cluster is $Cp*IrRu_3(\mu\text{-H})_4(CO)_9$, which was obtained in 5% yield from the reaction of $[Cp*IrCl_2]_2$ with $[PPN][Ru_3(CO)_9BH_4]$ [10]. We attempted to synthesize $Cp*IrRu_3$ clusters by reacting various Cp*Ir complexes with triruthenium clusters including: (i) the reaction of $Ru_3(CO)_{10}(NCCH_3)_2$ with $Cp*Ir(CO)_2$ at ambient temperature and also under photolytic conditions, which led only to decomposition of the $Ru_3(CO)_{10}(NCCH_3)_2$ [11], and (ii) ionic coupling between $[Cp*Ir(CH_3COCH_3)_3]^{2+}$ or $[Cp*Ir(CH_3CN)_3]^{2+}$ [12], with $[Ru_3(CO)_{11}]^{2-}$ [13], which afforded an intractable brown solid. It was reported that the reaction of $Cp*Rh(CO)_2$ or $CpRh(CO)_2$ with $Ru_3(CO)_{12}$ in the presence of hydrogen afforded the rhodium–ruthenium clusters $Cp*RhRu_3(\mu\text{-H})_2(CO)_{10}$ or $CpRhRu_3(\mu\text{-H})_2(CO)_{10}$, respectively [14]. We thus attempted to synthesize the iridium analogues by reacting $Ru_3(CO)_{12}$, **1**, with $Cp*Ir(CO)_2$, **2a**, or $CpIr(CO)_2$, **2b**, in the presence of molecular hydrogen.

The reaction of **1** with **2a** at 70–90 °C under a hydrogen flow afforded the clusters $Cp*IrRu_3(\mu\text{-H})_2(CO)_{10}$, **3a**, and $Cp*IrRu_3(\mu\text{-H})_4(CO)_9$, **4a**, in 40% and 13% yields, respectively (Scheme 1). The analogous reaction with **2b** afforded only the dihydrido species $CpIrRu_3(\mu\text{-H})_2(CO)_{10}$, **3b**, in 46% yield (w.r.t. consumed **1**); the tetrahydrido cluster, $CpIrRu_3(\mu\text{-H})_4(CO)_9$, **4b**, was not formed even after refluxing for 10 h. In contrast, when **3a** was treated with hydrogen (1 atm) for 6 h, it yielded **4a** in about 69% yield. However, quantitative conversion was not observed even after prolonged heating. The reverse reaction of **4a** under 1 atmosphere CO resulted in cluster fragmentation to **1** and **2a**. Such a breakdown of the cluster skeleton has also been reported for the rhodium analogue $Cp*RhRu_3(\mu\text{-}$

$H)_2(CO)_{10}$ [14]. Similarly, while **3a** is stable in air in the solid state for a few days, **3b** decomposed in a few hours to a black solid.

Clusters **3a**, **3b** and **4a** have all been completely characterized, including by single crystal X-ray crystallography; the ORTEPs with selected bond parameters are shown in Figs. 1–3, respectively.

The structures of **3a** and **3b** are similar except for a difference in the positions of the hydrides; the hydride positions are corroborated by the lengthening of the hydride-bridged metal–metal bond lengths [Ir(1)Ru(2) and Ru(2)Ru(4) in **3a**, and Ru(2)Ru(3) and Ru(3)Ru(4) in **3b**]. The hydride positions in **3a** and **3b** are similar to those in the related clusters $Cp*RhRu_3(\mu\text{-H})_2(CO)_{10}$ [14], and $CpRhRu_3(\mu\text{-H})_2(CO)_{10}$ and $CpIrOs_3(\mu\text{-H})_2(CO)_{10}$ [14,8a], respectively. Thus it appears that the positions of the hydrides are determined by whether it is a Cp or Cp* on the unique vertex. Both contain a bridging carbonyl each which persist in solution; the IR spectra show a bridging carbonyl vibration at 1788 and 1820 cm^{-1} for **3a** and **3b**,
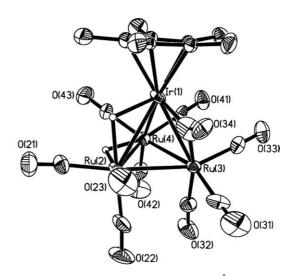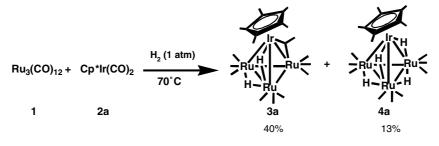

Fig. 1. ORTEP diagram and selected bond lengths (Å) and angles (°) for **3a**. Thermal ellipsoids are drawn at 50% probability level. Organic hydrogens are omitted for clarity. Ir(1)Ru(2) = 2.9082(12); Ir(1)Ru(3) = 2.7695(12); Ir(1)Ru(4) = 2.7659(12); Ru(2)Ru(3) = 2.7862(16); Ru(2)-Ru(4) = 2.8990(17); Ru(3)Ru(4) = 2.7612(18); Ir(1)C(34) = 1.983(19); Ru(3)-C(34) = 2.145(15); O(34)C(34) = 1.195(18); O(34)C(34)Ir(1) = 141.3(15); O(34)C(34)Ru(3) = 134.4(15); Ir(1)C(34)Ru(3) = 84.2(5).

$$Ru_3(CO)_{12} + Cp*Ir(CO)_2 \xrightarrow[\text{70°C}]{H_2\ (1\ atm)} \text{3a} + \text{4a}$$

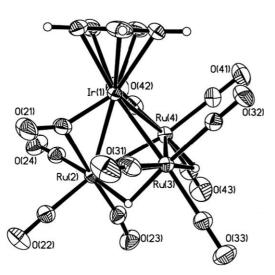| **1** | **2a** | | **3a** | **4a** |
| | | | 40% | 13% |

Scheme 1.

Fig. 2. ORTEP diagram and selected bond lengths (Å) and angles (°) for **3b**. Thermal ellipsoids are drawn at 50% probability level. Organic hydrogens are omitted for clarity. Ir(1)Ru(2) = 2.7788(2); Ir(1)Ru(3) = 2.7276(2); Ir(1)Ru(4) = 2.7077(2); Ru(2)Ru(3) = 2.9246(3); Ru(2)Ru(4) = 2.7433(3); Ru(3)Ru(4) = 2.8765(3); Ir(1)C(21) = 1.888(3); Ru(2)C(21) = 2.325(3); O(21)C(21) = 1.159(3); O(21)C(21)Ir(1) = 149.8(2); O(21)C(21)-Ru(2) = 128.3(2); Ir(1)C(21)Ru(3) = 81.85(9).
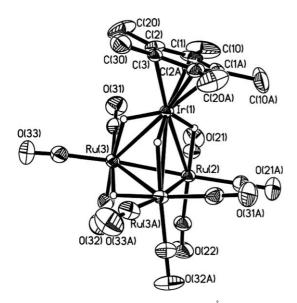

Fig. 3. ORTEP diagram and selected bond lengths (Å) and angles (°) for **4a**. Thermal ellipsoids are drawn at 50% probability level. Organic hydrogens are omitted for clarity. Ir(1)Ru(2) = 2.9480(5); Ir(1)Ru(3) = 2.9061(4); Ru(2)Ru(3) = 2.7652(6); Ru(3)Ru(3A) = 2.9400(7); Ru(3)Ir(1)Ru(3A) = 60.774(15); Ru(3)Ir(1)Ru(2) = 56.369(11); Ru(3)Ir(1)Ru(2) = 56.369(11); Ru(3)Ru(2)-Ru(3A) = 64.228(19); Ru(3)Ru(2)Ir(1) = 61.050(13); Ru(2)Ru(3)Ir(1) = 62.581(13); Ru(2)Ru(3)Ru(3A) = 57.886(9); Ir(1)Ru(3)Ru(3A) = 59.613(7).

respectively. Although both hydrides in **3a** and **3b** should be non-equivalent, the ambient temperature ^{1}H NMR spectra for both showed a single sharp hydride resonance (δ −18.21 and −17.84 ppm for **3a** and **3b**, respectively). On lowering the temperature, broadening of the hydride resonances were observed but no decoalescence was dis-

cernible down to 190 K, indicating rapid exchange of the hydrides.

Cluster **4a** is also stable in air only for a short period of time; slow decomposition to an insoluble black solid was observed after a few hours. As mentioned above, this cluster was previously reported as a by-product from a reaction, although the solid-state structure was not reported [10]. The solution IR spectrum showed bands only in the terminal carbonyl region, consistent with the solid-state structure. At room temperature, the ^{1}H NMR spectrum showed a singlet resonance at δ −18.59 ppm; on cooling, the hydride signal broadened but no decoalescence was observed down to 200 K, again demonstrating that the hydrides were in rapid exchange.
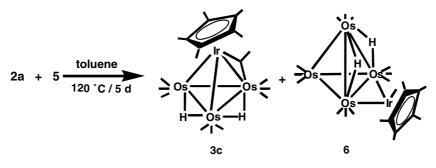
2.2. Iridium–osmium clusters

In the synthesis of analogous iridium–osmium clusters, it appears that the method of choice is via a condensation reaction between $Os_3(\mu\text{-}H)_2(CO)_{10}$, **5** [15], and the appropriate group 9 precursor. Examples prepared using this method include $CpCoOs_3(\mu\text{-}H)_2(CO)_{10}$ (33% yield), [3f] $Cp^*RhOs_3(\mu\text{-}H)_2(CO)_{10}$ (12% yield) and $Cp^*RhOs_3(\mu\text{-}H)_4(CO)_9$ (36% yield), [3i] and $CpIrOs_3(\mu\text{-}H)_2(CO)_{10}$ (21% yield) [8a]. Consequently we have also adopted this methodology as one of our synthetic routes.

The reaction of **2a** with **5** at 120 °C afforded the cluster $Cp^*IrOs_3(\mu\text{-}H)_2(CO)_{10}$, **3c**, in 70% yield together with a trace amount of the pentanuclear cluster $Cp^*IrOs_4(\mu\text{-}H)_2(CO)_{13}$, **6** (Scheme 2). Thus unlike in the rhodium analogue, where the reaction of $Cp^*Rh(CO)_2$ with **5** was found to give rise to not only the $RhOs_3$ cluster but also Rh_2Os_2 clusters, presumably via cluster fragmentation [3c], the reaction of **5** with **2a** is relatively clean, affording **3c** in high yield. Both clusters **3c** and **6** have been completely characterized including by single crystal X-ray crystallographic analyses. The ORTEP plots and selected bond parameters of **3c** and **6** are shown in Figs. 4 and 5, respectively.

Cluster **3c** is isostructural to **3b** and therefore the positions of the hydrides are in contrast to those found in the analogous Cp^*RhRu_3 and Cp^*IrRu_3 clusters; the hydride positions are again corroborated by the longer metal–metal bonds being the hydride-bridged ones (Os(2)Os(3) and Os(3)Os(4)). As for the iridium–ruthenium analogues, the bridging carbonyl persists in solution; the IR spectrum shows a broad absorption at 1782 cm^{-1}. However, the ^{1}H NMR spectrum at room temperature showed two broad resonances in the hydride region, which sharpened at 233 K to two resonances at δ −17.65 and −20.66 ppm. These resonances have been tentatively assigned as shown in Fig. 6 based on the earlier observations on related compounds that OsHOs cis to a carbonyl bridge have chemical shifts to higher field than one not cis to a bridging carbonyl [3f]. Presumably the exchange mechanism is the same as that for the $RhRu_3$ analogues [16].

Cluster **6** is structurally similar to $CpRhOs_4(\mu\text{-}H)_2(CO)_{13}$ reported earlier by Shore and coworkers [17].
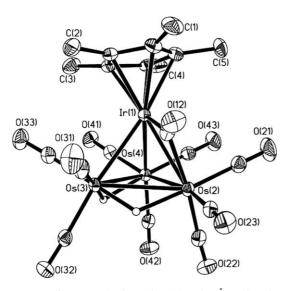
Scheme 2.

Fig. 4. ORTEP diagram and selected bond lengths (Å) and angles (°) for **3c**. Thermal ellipsoids are drawn at 50% probability level. Organic hydrogens are omitted for clarity. Ir(1)Os(2) = 2.7789(4); Ir(1)Os(3) = 2.7644(4); Ir(1)Os(4) = 2.7326(3); Os(2)Os(3) = 2.9656(4); Os(2)Os(4) = 2.7801(3); Os(3)Os(4) = 2.8855(4); Ir(1)C(12) = 1.910(5); Os(2)C(12) = 2.239(5); O(12)C(12) = 1.179(6); O(12)C(12)Ir(1) = 145.6(5); O(12)-C(12)Os(2) = 130.7(4); Ir(1)C(12)Os(2) = 83.7(2).
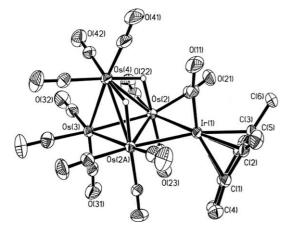

Fig. 6. Tentative ^{1}H NMR assignments for the hydrides in **3c**.

Although not identified, by comparison of the hydride resonance, we believe that the Cp analogue of **6**, viz., CpIrOs$_4$(μ-H)$_2$(CO)$_{13}$, may have been obtained (reported as band 2) by earlier workers from the analogous reaction of **2b** with **5** [8a]. The metal core of **6** consists of a tetrahedral Os$_4$ metal framework edge bridged by a Cp*IrCO fragment; consistent with the total valence electron count of 74. The shortest Os–Os bond is that bridged by the iridium

Fig. 5. ORTEP diagram and selected bond lengths (Å) and angles (°) for **6**. Thermal ellipsoids are drawn at 50% probability level. Organic hydrogens are omitted for clarity. Ir(1)Os(2) = 2.8109(3); Os(2)Os(2A) = 2.7764(4); Os(2)Os(3) = 2.8261(3); Os(2)Os(4) = 2.9459(3); Os(3)Os(4) = 2.7848(4); Ir(1)Os(2)Os(4) = 97.098(9); Ir(1)Os(2)Os(3) = 120.835(8); Os(2)Ir(1)Os(2A) = 59.190(10); Os(2A)Os(3)Os(2) = 58.842(10).
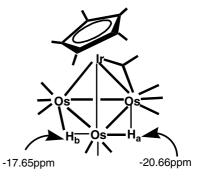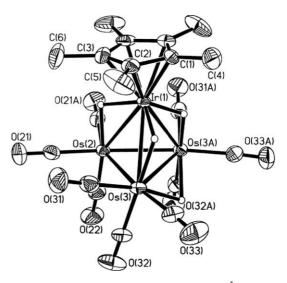

Fig. 7. ORTEP diagram and selected bond lengths (Å) and angles (°) for **4c**. Thermal ellipsoids are drawn at 50% probability level. Organic hydrogens are omitted for clarity. Ir(1)Os(2) = 2.9513(4); Ir(1)Os(3) = 2.9148(3); Os(2)Os(3) = 2.8013(4); Os(3)Os(3A) = 2.9799(5); Os(3)Os(2)-Os(3A) = 64.264(12); Os(3)Os(2)Ir(1) = 60.822(9).

fragment $[Os(2)Os(2A) = 2.7764(4)$ Å]. We have also ruled out the tetranuclear cluster $Os_4(\mu\text{-}H)_4(CO)_{12}$, which is often present as an impurity in $Os_3(\mu\text{-}H)_2(CO)_{10}$, as the precursor for **6**; the reaction of $Os_4(\mu\text{-}H)_4(CO)_{12}$ with **2a** under similar conditions afforded **6** in only trace amounts.

Hydrogenation of **3c** afforded the tetrahydrido species $Cp^*IrOs_3(\mu\text{-}H)_4(CO)_9$, **4c**, as a dark orange, air-stable, solid in 90% yield. The molecular structure has been confirmed by a single crystal X-ray crystallographic study, and shows that it is isostructural with **4a**; the ORTEP plot together with selected bond parameters are shown in Fig. 7.

The ^1H NMR spectrum of **4c** at room temperature showed a singlet at $\delta -19.27$ ppm, suggesting the fluxional nature of the hydrides. On cooling to 195 K a total of five resonances could be seen (Fig. 8). These resonances may be ascribed to the presence of two isomers in solution; their proposed structures and the tentative assignments are given in the inset to Fig. 8. From the NMR, isomer I is the major

isomer; this is consistent with that obtained in the solid state. A ^1H EXSY (Fig. 9) showed all 10 possible exchange crosspeaks among the hydride resonances, indicative of hydride exchange that results in isomerisation between the two isomers (intermolecular exchange) as well as hydride exchange within the same isomer (intramolecular exchange). A plausible set of exchanges which involve either single hydride migration, or two hydride migrations (either simultaneous or step-wise), that can account for the observed exchange crosspeaks is depicted in Scheme 3. The crosspeak labeled b–e can only be accounted for by a more complex exchange mechanism, and the weaker intensity compared to the others is consistent with that.

The reaction of **2a** with the "lightly stabilized" cluster $Os_3(CO)_{10}(CH_3CN)_2$, **7**, afforded the known trinuclear cluster $Cp^*IrOs_2(CO)_9$, **8** [8b], and the novel cluster $Cp^*IrOs_3(CO)_{11}$, **9**. Cluster **9** has been characterized spectroscopically as well as by a single crystal X-ray diffraction study;
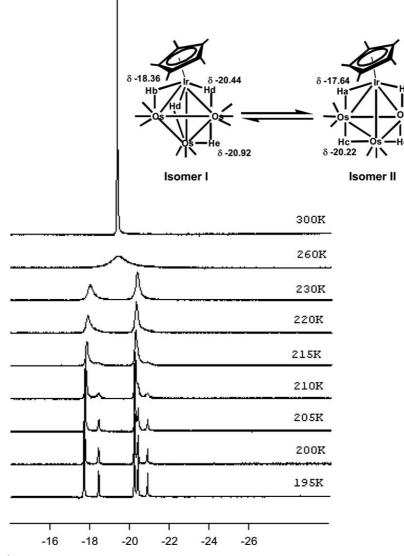

Fig. 8. Variable temperature ^1H NMR spectra (d_8-toluene) of **4c**. *Inset*. Proposed isomers and the tentative assignments of the ^1H resonances for the bridging hydrides.
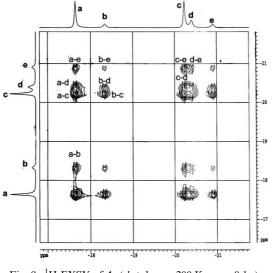
Fig. 9. ^{1}H EXSY of **4c** (d_8-toluene, 200 K, $\tau_m = 0.1$ s).

Fig. 10. ORTEP diagram and selected bond lengths (Å) and angles (°) for **9**. Thermal ellipsoids are drawn at 50% probability level. Organic hydrogens are omitted for clarity. Ir(1)Os(2) = 2.7803(6); Ir(1)Os(3) = 2.7734(7); Os(2)Os(2A) = 2.8137(8); Os(2)Os(3) = 2.7663(6); Ir(1)C(12) = 2.108(9); Os(2)C(12) = 2.058(9); O(12)C(12) = 1.172(11); O(12)C(12)-Os(2) = 144.2(7); O(12)C(12)Ir(1) = 132.1(7); Os(2)C(12)Ir(1) = 83.7(3).

the ORTEP plot, together with selected bond parameters, is given in Fig. 10. The overall structure of **9** is similar to that of the rhodium analogue, Cp*RhOs$_3$(CO)$_{11}$ [18]. The

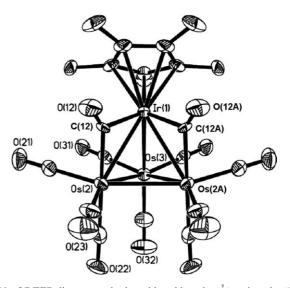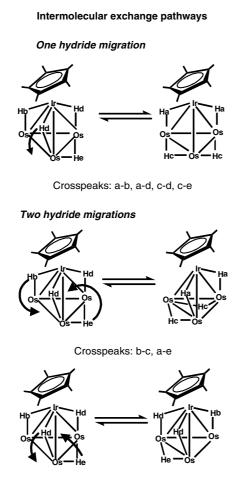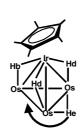**Intermolecular exchange pathways**

One hydride migration

Crosspeaks: a-b, a-d, c-d, c-e

Two hydride migrations

Crosspeaks: b-c, a-e

Crosspeaks: b-d, d-e

Intramolecular exchange pathways

Crosspeak: b-d

Crosspeak: a-c

Scheme 3.

tetrahedral metal core, with six metal–metal bonds, is as expected for a 60-electron metal cluster. There is a crystallographic mirror plane that passes through Ir(1), Os(3) and CO(32). Two bridging carbonyl ligands are found bridging the Ir(1)–Os(2) and Ir(1)–Os(2A) bonds; these bonds are marginally longer than the corresponding unbridged bond [Ir(1)Os(2) = 2.7803(6) Å cf Ir(1)Os(3) = 2.7734 (7) Å]. Interestingly, the bridging carbonyls are closer to the osmium [Ir(1)C(12) = 2.108(9) Å cf Os(2)C(12) = 2.058(9) Å], whereas it is the other way around in **3c** [Ir(1)C(12) = 1.910(5) Å cf Os(2)C(12) = 2.239(5) Å].

It was reported earlier that the reaction of **2a** with a cluster precursor closely related to **7**, viz., $Os_3(CO)_{10}$-$(COE)_2$ (COE = cyclooctene), afforded $Cp*(CO)IrOs_3$-$(CO)_{12}$, **10**, and not **9** [8d]. Indeed, monitoring of the reaction between **2a** and **7** showed that **9** was not formed directly in the reaction but has resulted from decarbonylation of **10** upon solvent removal from the crude reaction mixture under reduced pressure.

Clusters **3c**, **4c** and **9** form a series in which two of the bridging hydrides in **4c** are successively replaced by a bridging carbonyl in **3c** and then in **9**. We have already shown that hydrogenation of **3c** indeed afforded **4c**, and so it was of interest to see if **9** can be related to **3c** or **4c** in a similar manner. Attempts to convert cluster **3c** or **4c** to **9** by reaction with CO (100 psi) at 120 °C, and vice-versa with 100 psi of H_2 at 120 °C, did not lead to any conversion. In all the cases small amounts of insoluble solids were obtained after the reaction.

3. Concluding remarks

We have thus found that the reaction of **1** with **2a** or **2b** under a hydrogen atmosphere affords tetrahedral cyclopentadienyliridiumtriruthenium hydrido clusters in moderate yields. These clusters are generally moderately air-stable. In contrast, the analogous reactions of **2a** with suitable triosmium precursors afford tetrahedral cyclopentadienyliridiumtriosmium clusters in good to excellent yields, and these are generally air-stable. The relative stability between these two classes of heterometallic clusters no doubt is a reflection of the well-established chemistry of ruthenium and osmium clusters. Similarly, the hydride ligands in the iridium–ruthenium series are highly fluxional; decoalescence are typically not reached even down to 200 K. In comparison, decoalescence can be observed at fairly easily attainable temperatures in the iridium–osmium systems.

4. Experimental

4.1. General procedures

All reactions and manipulations were carried out under nitrogen using standard Schlenk techniques. Solvents were purified, dried, distilled and stored under nitrogen prior to use. High pressure reactions were carried out in a Parr screw-cap bomb of 60 ml capacity. The products were gen-

erally separated by column chromatography on silica gel 60 (230–430 mesh ASTM) or by thin-layer chromatography (TLC), using plates coated with silica gel 60 F254 of 0.25 or 0.5 mm thickness and extracted with hexane or dichloromethane. Routine NMR spectra were recorded on a BRUKER ACF-300 FT NMR spectrometer. [1]H chemical shifts reported are referenced against the residual proton signals of the solvents. Selective decoupling experiments, spin saturation transfer and 2D spectra (EXSY, NOESY) were acquired on a Bruker Avance DRX500 or Bruker AMX500 machine. Mass spectra were obtained on a Finnigan MAT95XL-T spectrometer in an *m*-nitrobenzyl alcohol matrix. Microanalyses were carried out by the microanalytical laboratory at the National University of Singapore. The precursors $Cp*Ir(CO)_2$, **2a** [19], $CpIr(CO)_2$, **2b** [20], $Os_3(\mu\text{-}H)_2(CO)_{10}$, **5** [19], and $Os_3(CO)_{10}(CH_3CN)_2$, **7** [21], were prepared according to the literature methods. All other reagents were from commercial sources and used as supplied.

4.2. Reaction of 1 with 2a

A steady stream of hydrogen gas was bubbled through a solution of **1** (114.7 mg; 0.18 mmol) and **2a** (68.9 mg; 0.18 mmol) in heptane (60 ml) at 70 °C for 1.25 h. The solution turned dark red during this period. After cooling to room temperature, chromatographic separation on silica gel with hexane as eluant gave a broad orange yellow band consisting of unreacted **1** and $Ru_4(\mu\text{-}H)_4(CO)_{12}$ (60 mg, identified by its IR spectrum). This was followed by an orange band of $Cp*IrRu_3(\mu\text{-}H)_4(CO)_9$, **4a**, (yield = 15.4 mg, 9.7%) and a deep red band of $Cp*IrRu_3(\mu\text{-}H)_2(CO)_{10}$, **3a**, (yield = 48.4 mg, 30%). Both **3a** and **4a** were recrystallized from hexane at −30 °C.

3a. IR (hex): ν_{CO} 2081m, 2061s, 2051m, 2041vs, 2003s, 1966w, 1788m cm⁻¹. ^{1}H NMR (d_8-toluene): δ 1.78 (s, 15H, Cp*), −18.20 (s, 2H, MHM). FAB-MS: *m/z* 911.8 (M⁺). Calculated for $C_{20}H_{17}IrO_{10}Ru_3$: C, 26.31; H, 1.87%. Found: C, 26.58; H, 1.48%.

4a. IR (hex): ν_{CO} 2080s, 2066s, 2048vs, 2025s, 2008m,sh, 1988m, 1954w cm⁻¹. ^{1}H NMR (d_8-toluene): δ 1.79 (s, 15H, Cp*), −18.59 (s, 4H, MHM). FAB-MS: *m/z* 887.6 (M⁺). Calculated for $C_{19}H_{19}IrO_9Ru_3 \cdot 1/4$toluene: C, 27.28; H, 2.32%. Found: C, 26.90; H, 1.92%.

4.3. Reaction of 1 with 2b

A steady stream of hydrogen gas was bubbled through a solution of **1** (114.8 mg; 0.18 mmol) and excess **2b** in hexane (60 ml) for 2 h. The yellow orange solution turned dark brown during this period. After cooling to room temperature chromatographic separation of the reaction mixture on a silica gel column afforded a yellow band which consisted of unreacted **1** mixed with $Ru_4(\mu\text{-}H)_4(CO)_{12}$ (55 mg). Further elution with hexane gave a deep red band, which on evaporation yielded $CpIrRu_3(\mu\text{-}H)_2(CO)_{10}$, **3b**, (yield = 45.8 mg, 30%).

3b. IR (hex): ν_{CO} 2088m, 2067vs, 2047vs, 2020m, 2009s, 2002sh, 1976w, 1820w cm^{-1}. ^{1}H NMR (CDCl$_3$): δ 4.84 (s, 5H, Cp), −17.84 (s, 2H, MHM). FAB-MS: m/z 842.4 (M$^+$). We were not able to obtain satisfactory elemental analyses as it decomposed rapidly.

4.4. Reaction of 3a with hydrogen

A hexane solution (20 ml) of cluster **3a** (5 mg, 0.005 mmol) was refluxed, while a steady stream of hydrogen gas was bubbled through, for 6 h in a three-necked round-bottomed flask. Separation of the reaction mixture by TLC, eluting with hexane, gave **4a** (yield = 3.4 mg, 69%) and a trace amount of **3a**, both identified by IR spectroscopy.

4.5. Reaction of 4a with CO

A hexane solution (5 ml) of **4a** (5 mg, 0.005 mmol) was stirred under CO (1 atm) at ambient temperature. IR spectrum of the reaction mixture showed quantitative conversion to **1** and **2a** within 5 h.

4.6. Reaction of 2a with 5

Cluster **5** (250.3 mg, 0.29 mmol) together with **2a** (112.5 mg, 0.29 mmol) and toluene (20 ml) were placed in a Carius tube fitted with a Teflon valve, degassed with three freeze–pump–thaw cycles, and then heated at 120 °C for 5 d. During this period the CO generated was pumped away once every 24 h. At the end of the reaction, the volatile compounds were removed under reduced pressure and the residue redissolved in the minimum amount of a hexane–toluene mixture and subjected to column chromatography. Elution with hexane yielded an orange-red band identified as Cp*IrOs$_3$(μ-H)$_2$(CO)$_{10}$, **3c**, (yield = 244.8 mg, 70.7%) and continuing with hexane/dichloromethane (1:4, v/v) yielded a pink band of Cp*IrOs$_4$(μ-H)$_2$(CO)$_{13}$, **6a**, in trace amounts (yield = 3 mg, <1%).

3c. IR (hex): ν_{CO} 2085m, 2065s, 2040vs, 2006m, 2000vs, 1967w, 1959mw, 1782br cm^{-1}. ^{1}H NMR (d_8-toluene, 233 K): δ 1.60 (s, Cp*), −17.65 (s, OsHOs), −20.66 (s, OsHOs). FAB–MS: m/z 1180.8 (M$^-$). Calculated for C$_{20}$H$_{15}$IrO$_{10}$Os$_3$: C, 20.33; H, 1.44%. Found: C, 20.54; H, 1.55%.

6a. IR (CH$_2$Cl$_2$): ν_{CO} 2081m, 2067s, 2050s, 2030m, 1955w cm^{-1}. ^{1}H NMR (CDCl$_3$): δ 1.85 (s, Cp*), −19.74 (s, OsHOs). FAB-MS: m/z 1370.4 (M$^-$ − 3CO).

4.7. Reaction of 3c with H$_2$

A hexane solution (6 ml) of **3c** (59.9 mg, 0.05 mmol) was placed in a Parr bomb, pressurized with H$_2$ (100 psi) and heated at 120 °C for 24 h. The colour of the solution changed from red to bright orange. TLC separation of the mixture with 100% hexane yielded the cluster Cp*Ir-Os$_3$(μ-H)$_4$(CO)$_9$, **4c** (yield = 52.8 mg, 90.1%).

4c: IR (hex): ν_{CO} 2084s, 2053vs, 2047vs, 2025w, 2005vs, 1992m, 1983vs, 1947w cm^{-1}. ^{1}H NMR (d_8-toluene, 300 K): δ 1.57 (s, Cp*), −19.27 (s, 4H, MHM). FAB-MS: m/z 1154.8 (M$^-$). Calculated for C$_{19}$H$_{19}$IrO$_9$Os$_3$: C, 19.76; H, 1.64%. Found: C, 20.09; H, 1.59%.

4.8. Reaction of 2a with 7

A solution of **7** (80 mg, 0.085 mmol) in CH$_2$Cl$_2$ (10 ml) was cannula transferred into a solution of **2a** (32.8 mg, 0.085 mmol) in CH$_2$Cl$_2$ (10 ml). A colour change from yellow to red occurred immediately. After stirring at room temperature for 1 h, the solvent was removed on the vacuum line and the residue so obtained was redissolved in the minimum volume of dichloromethane and chromatographed on silica-gel TLC plates. Elution with hexane/dichloromethane (9/1, v/v) gave one major band and two minor bands. Band 1 gave orange crystals of Cp*IrOs$_2$-(CO)$_9$, **8**, (trace amount) identified by comparison with the X-ray, IR, ^{1}H NMR and FAB data reported [8b]. Band 2 gave unreacted **2a**, and band 3 gave brown crystals of Cp*IrOs$_3$(CO)$_{11}$, **9** (yield = 21 mg, 20%).

9: IR (CH$_2$Cl$_2$): ν_{CO} 2072s, 2033vs, 2025s, 1996w, 1980m, 1837m cm^{-1}. ^{1}H NMR (CDCl$_3$): δ 2.07 (s, Cp*). FAB-MS: m/z 1208 (M$^+$), 1179 ([M − CO]$^+$), 1150 ([M − 2CO]$^+$), 1122 ([M − 3CO]$^+$), 1094 ([M − 4CO]$^+$), 1066 ([M − 5CO]$^+$), 1038 ([M − 6CO]$^+$). Calculated for C$_{21}$H$_{15}$IrO$_{11}$Os$_3$: C, 21.27; H, 1.54%. Found: C, 20.89; H, 1.24%.

4.9. Reaction of 4c with CO

A hexane solution (6 ml) of **4c** (10 mg) was placed in a Parr bomb, pressurized with CO (100 psi), and heated at 120 °C for 6 h. TLC separation of the mixture with 100% hexane afforded unreacted **4c** (yield = 2 mg, 20%) and **3c** (yield = 7 mg, 68%).

4.10. X-ray crystal structure determinations

Crystals were grown from dichloromethane/hexane solutions and mounted on quartz fibres. X-ray data were collected on a Bruker AXS APEX system, using Mo Kα radiation, at 223 K with the SMART suite of programs [22]. Data were processed and corrected for Lorentz and polarisation effects with SAINT [23], and for absorption effects with SADABS [24]. Structural solution and refinement were carried out with the SHELXTL suite of programs [25]. Crystal and refinement data are summarised in Tables 1 and 2.

The structures were solved by direct methods to locate the heavy atoms, followed by difference maps for the light, non-hydrogen atoms. All non-hydrogen atoms were generally given anisotropic displacement parameters in the final model. Organic hydrogen atoms were placed in calculated positions and refined with a riding model. The metal hydrides were all located in the difference maps, except for

Table 1
Crystal and refinement data for **3a–c**

Compound	3a	3b	3c
Empirical formula	$C_{20}H_{17}IrO_{10}Ru_3$	$C_{15}H_7IrO_{10}Ru_3$	$C_{20}H_{17}IrO_{10}Os_3$
Formula weight	912.75	842.62	1180.14
Crystal system	Monoclinic	Orthorhombic	Triclinic
Space group	$P2_1/n$	$Pbca$	$P\bar{1}$
a (Å)	8.7203(4)	14.8001(9)	9.5705(11)
b (Å)	14.4647(7)	15.1152(9)	10.4175(12)
c (Å)	19.7560(9)	17.6179(10)	12.4073(15)
α (°)	90	90	84.465(2)
β (°)	97.229(2)	90	88.361(2)
γ (°)	90	90	76.665(2)
Volume (Å^3)	2472.1(2)	3941.2(4)	1198.0(2)
Z	4	8	2
Density (calculated) (Mg/m^3)	2.452	2.840	3.271
Absorption coefficient (mm^{-1})	7.214	9.037	21.446
$F(000)$	1704	3088	1044
Crystal size (mm^3)	$0.16 \times 0.14 \times 0.01$	$0.30 \times 0.26 \times 0.08$	$0.26 \times 0.10 \times 0.04$
Θ range for data collection (°)	2.08–24.71	2.25–30.04	2.02–30.06
Reflections collected	17513	60014	18224
Independent reflections [R_{int}]	4213 [0.0463]	5760 [0.0290]	6813 [0.0342]
Max. and min. transmission	0.931 and 0.392	0.532 and 0.172	0.481 and 0.072
Data/restraints/parameters	4213/0/287	5760/0/290	6813/0/320
Goodness-of-fit on F^2	1.226	1.116	1.017
Final R indices [$I > 2\sigma(I)$]	$R_1 = 0.0617$, $wR_2 = 0.1288$	$R_1 = 0.0176$, $wR_2 = 0.0435$	$R_1 = 0.0265$, $wR_2 = 0.0635$
R indices (all data)	$R_1 = 0.0699$, $wR_2 = 0.1320$	$R_1 = 0.0197$, $wR_2 = 0.0441$	$R_1 = 0.0315$, $wR_2 = 0.0654$
Largest diff. peak and hole (e Å^{-3})	4.486 and −2.806	0.595 and −1.097	2.433 and −1.556

Table 2
Crystal and refinement data for **4a**, **4c**, **6** and **9**

Compound	4a	4c	6	9
Empirical formula	$C_{19}H_{19}IrO_9Ru_3$	$C_{19}H_{19}IrO_9Os_3$	$C_{23}H_{17}IrO_{13}Os_4$	$C_{21}H_{15}IrO_{11}Os_3$
Formula weight	886.75	1154.14	1454.37	1206.13
Crystal system	Monoclinic	Monoclinic	Orthorhombic	Orthorhombic
Space group	$P2_1/m$	$P2_1/m$	$Pnma$	$Pnma$
a (Å)	8.4923(5)	8.4877(2)	18.0156(3)	17.6000(17)
b (Å)	15.7031(8)	15.7727(4)	13.8807(3)	13.9732(13)
c (Å)	9.8804(5)	9.8993(3)	11.5849(2)	10.0040(10)
α (°)	90	90	90	90
β (°)	110.129(3)	110.381(1)	90	90
γ (°)	90	90	90	90
Volume (Å^3)	1237.13(11)	1242.29(6)	2897.03(9)	2460.3(4)
Z	2	2	4	4
Density (calculated) (Mg/m^3)	2.380	3.085	3.334	3.256
Absorption coefficient (mm^{-1})	7.201	20.675	22.119	20.893
$F(000)$	828	1020	2560	2136
Crystal size (mm^3)	$0.12 \times 0.06 \times 0.05$	$0.22 \times 0.10 \times 0.04$	$0.14 \times 0.12 \times 0.08$	$0.16 \times 0.06 \times 0.03$
Θ range for data collection (°)	2.55–30.01	2.19–28.28	2.09–26.37	2.31–26.37
Reflections collected	10789	10624	30673	19877
Independent reflections [R_{int}]	3427 [0.0310]	3177 [0.0357]	3098 [0.0342]	2618 [0.0632]
Max. and min. transmission	0.715 and 0.479	0.492 and 0.092	0.271 and 0.148	0.573 and 0.135
Data/restraints/parameters	3427/2/165	3177/5/163	3098/0/208	2618/0/175
Goodness-of-fit on F^2	1.057	1.046	1.109	1.155
Final R indices [$I > 2\sigma(I)$]	$R_1 = 0.0327$, $wR_2 = 0.0696$	$R_1 = 0.0277$, $wR_2 = 0.0644$	$R_1 = 0.0211$, $wR_2 = 0.0485$	$R_1 = 0.0374$, $wR_2 = 0.0692$
R indices (all data)	$R_1 = 0.0364$, $wR_2 = 0.0711$	$R_1 = 0.0329$, $wR_2 = 0.0661$	$R_1 = 0.0237$, $wR_2 = 0.0496$	$R_1 = 0.0457$, $wR_2 = 0.0715$
Largest diff. peak and hole (e Å^{-3})	1.783 and −0.760	2.428 and −1.575	1.057 and −0.822	1.561 and −1.784

those in **3a** which were placed in calculated positions using XHYDEX [26]; the atomic parameters were either refined fully (**3b**, **3c**, **6**) or with fixed isotropic thermal parameter and restrained (**4a** and **4c**) or riding on one of the heavy atoms (**3a**).

4.11. Supplementary material

Crystallographic data (excluding structure factors) for the structures in this paper have been deposited with the Cambridge Crystallographic Data Centre as supplementary

Acknowledgements

References

[1] (a) R.D. Adams, B. Captain, J. Organomet. Chem. 689 (2004) 4521;
(b) P. Braunstein, J. Rosé, in: R.D. Adams, F.A. Cotton (Eds.), Catalysis by Di and Polynuclear Metal Cluster Complexes, Wiley-VCH, New York, 1998;
(c) E.W. Abel, F.G.A. Stone, G. Wilkinson (Eds.), Comprehensive Organometallic Chemistry II, Pergamon, Oxford, 1995;
(d) G. Wilkinson, F.G.A. Stone, E.W. Abel (Eds.), Comprehensive Organometallic Chemistry, Pergamon, Oxford, 1982.

[2] G. Süss-Fink, G. Meister, Adv. Organomet. Chem. 35 (1993) 41.

[3] For examples: (a) S. Haak, G. Süss-Fink, A. Neels, H. Stoeckli-Evans, Polyhedron 18 (1999) 1675;
(b) A.A. Koridze, A.M. Sheloumov, F.M. Dolgushin, A.I. Yanovsky, Yu.T. Struchkov, P.V. Petrovskii, J. Organomet. Chem. 536/537 (1997) 381;
(c) D.Y. Jan, L.Y. Hsu, W.L. Hsu, S.G. Shore, Organometallics 6 (1987) 274;
(d) L.Y. Hsu, W.L. Hsu, D.Y. Jan, A.G. Marshall, S.G. Shore, Organometallics 3 (1984) 591;
(e) S.G. Shore, W.L. Hsu, M.R. Churchill, C. Bueno, J. Am. Chem. Soc. 105 (1983) 655;
(f) M.R. Churchill, C. Bueno, S. Kennedy, J.C. Bricker, J.S. Plotkin, S.G. Shore, Inorg. Chem. 21 (1982) 627;
(g) S.G. Shore, W.L. Hsu, C.R. Weisenberger, M.L. Caste, M.R. Churchill, C. Bueno, Organometallics 1 (1982) 1405;
(h) M.R. Churchill, C. Bueno, W.L. Hsu, J.S. Plotkin, S.G. Shore, Inorg. Chem 21 (1982) 1958;
(i) J.S. Plotkin, D.G. Alway, C.R. Weisenberger, S.G. Shore, J. Am. Chem. Soc. 102 (1980) 6156;
(j) L.J. Farrugia, J.A.K. Howard, P. Mitrprachachon, J.L. Spencer, F.G.A. Stone, P. Woodward, J. Chem. Soc., Chem. Commun. (1978) 260.

[4] Some reviews on ruthenium catalysis are: (a) C. Bruneau, Top. Organomet. Chem. 11 (2004) 125;
(b) B. Schmidt, Eur. J. Org. Chem. (2004) 1865;
(c) M. Mori, J. Mol. Catal. A 213 (2004) 73;
(d) T. Kondo, T. Mitsudo, Curr. Org. Chem. 6 (2002) 1163;
(e) B.M. Trost, F.D. Toste, A.B. Pinkerton, Chem. Rev. 101 (2001) 2067;
(f) T. Naota, H. Takaya, S. Murahashi, Chem. Rev. 98 (1998) 2599.

[5] For example: (a) D. Polet, A. Alexakis, Org. Lett. 7 (2005) 1621;
(b) A. Haynes, P.M. Maitlis, G.E. Morris, G.J. Sunley, H. Adams, P.W. Badger, C.M. Bowers, D.B. Cook, P.I.P. Elliott, T. Ghaffar, H. Green, T.R. Griffin, M. Payne, J.M. Pearson, M.J. Taylor, P.W. Vickers, R.J. Watt, J. Am. Chem. Soc. 126 (2004) 2847;
(c) J.-Y. Cho, M.K. Tse, D, Holmes, R.E. Maleczka Jr., M.R. Smith III, Science 295 (2002) 305;
(d) J.H. Jones, Platinum Metals Rev. 44 (2000) 94;
(e) R. Takeuchi, Polyhedron 19 (2000) 557;
(f) D.M. Tellers, R.G. Bergman, J. Am. Chem. Soc. 122 (2000) 954;
(g) S.E. Bromberg, T. Lian, R.G. Bergman, C.B. Harris, J. Am. Chem. Soc. 118 (1996) 2069.

[6] (a) G. Süss-Fink, S. Haak, V. Ferrand, H. Stoeckli-Evans, J. Mol. Catal. A 143 (1999) 163;
(b) G. Süss-Fink, S. Haak, V. Ferrand, H. Stoeckli-Evans, J. Chem. Soc., Dalton Trans. (1997) 3861.

[7] (a) G. Laurenczy, I. Dellavia, R. Roulet, ACH – Models Chem. 136 (1999) 317;
(b) A.U. Häerköenen, M. Ahlgrén, T.A. Pakkanen, J. Pursiainen, Organomet. Chem. 573 (1999) 225;
(c) A.U. Häerköenen, M. Ahlgrén, T.A. Pakkanen, J. Pursiainen, Organometallics 16 (1997) 689;
(d) A.U. Häerköenen, M. Ahlgrén, T.A. Pakkanen, J. Organomet. Chem. 530 (1997) 191.

[8] (a) L.Y. Hsu, W.L. Hsu, D.A. McCarthy, J.A. Krause, J.H. Chung, S.G. Shore, J. Organomet. Chem. 426 (1992) 121;
(b) A. Riesen, F.W.B. Einstein, A.K. Ma, R.K. Pomeroy, J.A. Shipley, Organometallics 10 (1991) 3629;
(c) P. Sundberg, B. Noren, B.F.G. Johnson, J. Lewis, P.R. Raithby, J. Organomet. Chem. 353 (1988) 383;
(d) V.J. Johnston, F.W.B. Einstein, R.K. Pomeroy, J. Am. Chem. Soc. 109 (1987) 7220.

[9] (a) L.J. Pereira, K.S. Chan, W.K. Leong, J. Organomet. Chem. 690 (2005) 1033;
(b) L. Pereira, W.K. Leong, S.Y. Wong, J. Organomet. Chem. 609 (2000) 104;
(c) L. Pereira, W.K. Leong, submitted.

[10] J.R. Galsworthy, C.E. Housecroft, D.M. Matthews, R. Ostrander, A.L. Rheingold, J. Chem. Soc., Dalton Trans. (1994) 69.

[11] G.A. Foulds, B.F.G. Johnson, J. Lewis, J. Organomet. Chem. 296 (1985) 147.

[12] (a) C. White, A. Yates, P.M. Maitlis, D.M. Heinekey, Inorg. Synth. 29 (1992) 228;
(b) H. Amouri, C. Guyard-Duhayon, J. Vaissermann, M.N. Rager, Inorg. Chem. 41 (2002) 1397.

[13] C.C. Nagel, J.C. Bricker, D.G. Alway, S.G. Shore, J. Organomet. Chem. 219 (1981) C9.

[14] W.E. Lindsell, C.B. Knobler, H.D. Kaesz, J. Organomet. Chem. 296 (1985) 209.

[15] H. Kaesz, Inorg. Synth. 28 (1990) 238.

[16] W.E. Lindsell, N.M. Walker, A.S.F. Boyd, J. Chem. Soc., Dalton Trans. (1988) 675.

[17] A. Colombie, D.A. McCarthy, J. Krause, L.Y. Hsu, W.L. Hsu, D.Y. Jan, S.G. Shore, J. Organomet. Chem. 383 (1990) 421.

[18] S.Y.-W. Hung, W.-T. Wong, J. Organomet. Chem. 580 (1999) 48.

[19] R.G. Ball, W.A.G. Graham, D.M. Heinekey, J.K. Hoyano, A.D. McMaster, B.M. Mattson, S.T. Michel, Inorg. Chem. 29 (1990) 2023.

[20] E.O. Fischer, K.S. Brenner, Zeit. Nat. 17b (1962) 774.

[21] J.N. Nicholls, M.D. Vargas, Inorg. Synth. 28 (1990) 232.

[22] SMART version 5.628, Bruker AXS Inc., Madison, WI, USA, 2001.

[23] SAINT version 6.22a, Bruker AXS Inc., Madison, WI, USA, 2001.

[24] G.M. Sheldrick, SADABS, 1996.

[25] SHELXTL version 5.1, Bruker AXS Inc., Madison, WI, USA, 1997.

[26] A.G. Orpen, XHYDEX: a program for locating hydrides in metal complexes, School of Chemistry, University of Bristol, UK, 1997.